including serum and seminal plasma [10–13]. Most of the LPA actions are mediated by G protein-coupled receptors (GPCR), termed LPA1/EDG2, LPA2/EDG4, and LPA3/EDG7, which belong to the endothelial differentiation gene (EDG) family [14,15].

LPA receptors are not only involved in normal development [16], but are also involved in proliferation and survival of many cancer cells [17–20]. For example, in the androgen-independent human prostate cancer PC-3 cells, LPA1 mediates LPA-regulated mitogenic signaling, whereas LPA2 and/or LPA3 appear to mediate cell survival [18]. In BPH, LPA has also been found to stimulate the growth of smooth muscle cells [21]. Previously, we reported that LPA promotes cell proliferation of normal prostatic cells, suggesting a potential importance of this signaling mechanism in BPH [22].

LPA can be generated in the extracellular milieu from lysophosphatidylcholine by the ectoenzyme autotaxin/lysophospholipase D (ATX/lyso PLD). Interestingly, ATX was first discovered as a tumor motility factor [23]. Another potential pathway for the synthesis of LPA is through the phosphorylation of monoacylglycerols by a recently identified lipid kinase called acylglycerol kinase (AGK). Overexpression of AGK in prostate cancer cells induced the formation and secretion of LPA, leading to increased cell growth [24]. On the other hand, we have recently reported that degradation of LPA in seminal plasma is mediated by prostatic acid phosphates (PAP), which is critical for regulating proliferation and androgen responsiveness of human prostate cells [25–27].

Considered together, these emerging data indicate that LPA is involved in the initiation and progression of prostate cancer and BPH and that, the balance between the synthesis and metabolism of LPA in the prostate

may be critical in maintaining normal prostatic micro-environment. In this study, surgical prostates were dissected using laser capture microdissection and the levels of LPA1, LPA2, LPA3, ATX, AGK and PAP mRNA in epithelial and the corresponding stromal cells of BPH, high grade prostatic intraepithelial neoplasia (HGPIN) and prostate cancer were quantitatively analyzed.

MATERIALS AND METHODS

Patients and Prostate Samples

Prostate tissue samples were obtained from 10 patients with newly diagnosed, clinically localized prostate cancer. The clinical characteristics of the patients are shown in Table I. Median age was 70.5 years, and median preoperative serum PSA was 9.5 ng/ml. No participant received previous hormonal ablation therapy, chemotherapy or radiotherapy. For control samples, prostate tissues without malignant neoplasia were obtained from 7 male patients with infiltrative bladder cancer (median age was 76 years ranging from 52 to 84). The age difference between the prostate cancer and bladder cancer group was not significant.

Cell Lines

Prostate cancer cell lines LNCaP, PC-3, and Du-145 were purchased from the American Type Culture Collection (Rockville, MD) and were maintained in RPMI 1640 plus 10% FCS (Life Technologies, Inc.). The cells were harvested at the exponential growing phase and subjected to the following RNA extraction.

TABLE I. Profile of Prostate Cancer Patients

Patient No.	Age (years)	PSA (ng/ml)	Gleason Sum	Gleason grade of captured cancer	p-Stage	Benign gland captured	Hyperplasia captured	HG-PIN captured	Cancer captured
1	60	37.5	9	5	T2bN0	+	+	−	+
2	62	8.7	7	3	T2bN0	+	+	−	+
3	73	4.7	6	3	T2bN0	+	+	−	+
4	65	18.0	7	4	T2bN0	+	+	+	+
5	63	4.7	6	3	T2bN0	+	+	−	+
6	73	19.9	9	4	T2bN0	+	−	−	+
7	73	9.4	8	3	T2bN0	+	−	+	+
8[a]	73	11.2	6	−	T2bN0	+	−	−	−
9	78	5.0	7	4	T2bN0	+	−	+	+
10	68	9.7	8	5	T2bN0	+	−	+	+

[a]Cancer was not captured in this sample due to a small cancer area but was confirmed in the following routine histological examination.

The Prostate

Specimen Preparation and Laser-Capture Microdissection (LCM)

Immediately after radical prostatectomy or radical cysto-prostatectomy, 5-mm-thick slices of the prostate tissue samples were prepared from several areas including major cancer foci (only from the prostate cancer patients) and the transition zone far from cancer foci in each individual. Tissue slices were fixed in freshly prepared methacarn consisting of 60% (v/v) absolute methanol, 30% chloroform, and 10% glacial acetic acid, dehydrated, and embedded in paraffin as described elsewhere [28]. This study complies with the Declaration of Helsinki and was approved by the institutional ethical committee. Written informed consent was obtained from all patients.

Tissue blocks were sectioned at 7 µm and mounted on a non-coating glass slide and then dried at room temperature for no more than 3 hr. Sections were deparaffinized and stained with Cresyl Violet using LCM Staining Kit (Ambion, Austin, TX) and then dehydrated in 100% ethanol followed by xylenes according to the manufacturer's protocol. LCM was performed with a PixCell II Microscope (Arcturus Engineering, Mountain View, CA) under a capture setting of 15-µm spot size, 1.5 msec pulse, and 55–75 mW beam. Epithelial cells within histologically benign glands and cancer foci were captured from all prostate cancer patients while hyperplastic nodules and HGPIN area were captured from five and four patients, respectively (Table I). Stromal cells around each dissected epithelial component were simultaneously captured. For normal control prostates, only benign glands and surrounding stroma were dissected. Photographs were taken of sections before and after LCM and assessed to confirm the histology of the laser captured cells (Fig. 1). Each laser capture session lasted no longer than 30 min to minimize RNA degradation.

RNA Extraction and Real-Time RT-PCR

Cells were lysed and RNA was isolated using the RNAqueous-Micro RNA Isolation Kit (Ambion) following the manufacturer's recommendations. RNA samples were treated with DNase using the Invitrogen DNase I (Invitrogen, Carlsbad, CA), and cDNA was synthesized as described elsewhere [29]. The housekeeping gene glyceraldehyde-3-phosphate dehydrogenase (GAPDH) was amplified using synthesized cDNA to confirm integrity.

To provide a reference standard RNA for use realtime reverse-transcription PCR (RT-PCR) total RNA was isolated from LNCap DU-145 and PC-3 cell lines using Trizol (Invitrogen) following the manufacturer's protocol.

Primers for LPA1, LPA2, LPA3, and AGK were described elsewhere [24,30], while primers for ATX were as follows: forward, GGGTGAAAGCTGGAA-CATTCTT; reverse, GAAGGCCTCTCATGATCTGG. Real-time PCR was conducted on a LightCycler system (Roche Diagnostics, Indianapolis, IN). Reaction mixture in 20 µl were amplified for 40 cycles using: 95 for 10 sec, 65–67°C for 10 sec and 72°C for 15 sec. GAPDH was determined with a ready-to-use LightCycler-h-GAPDH Housekeeping Gene Set (Roche Applied Science). Fluorescence data was analyzed with reference to the standard curve in each experiment. A melting curve analysis was always included to certify amplification. Target gene expression was related to GAPDH mRNA for normalization. All tests were conducted in duplicate to ensure reproducibility. The specificity of desired products in real-time PCR was also confirmed by conventional PCR using the same primer pairs as described elsewhere [29].

Immunohistochemical Staining of LPA3, ATX, and AGK

Protein expression of LPA 3, ATX, and AGK was examined by immunohistochemical staining for the same surgical specimens that were subjected to the laser capture microdissection described above. The anti-LPA3 monoclonal antibody and anti-ATX monoclonal antibody were kindly provided by Dr. Junken Aoki (Tohoku University Graduate School of Pharmaceutical Sciences). Details as to establishment of the anti-ATX monoclonal antibody and the anti-LPA3 monoclonal antibody were respectively described elsewhere [27,31]. The anti-AGK polyclonal antibody, OB0680, was newly developed from sera of rabbit that was immunized with a synthetic peptide. Amino acid sequence of the peptide was CDPRKREQMLTSPTQ that corresponded to codon 408–422 of C-terminal region of AGK. Immunohistochemical staining was carried out by the avidin–biotin method using peroxidase ABC kit (Vector Laboratories, Burlingame, CA).

Statistical Analysis

Comparisons between groups were made using the Student's t test or paired two-sample t tests. Two-sided $P < 0.05$ was considered significant.

RESULTS

Expression Profiles of Genes Related to LPA in Prostate Cancer Cells

The mRNAs corresponding to the LPA receptors (LPA1-3), LPA producing enzymes (ATX, AGK), and
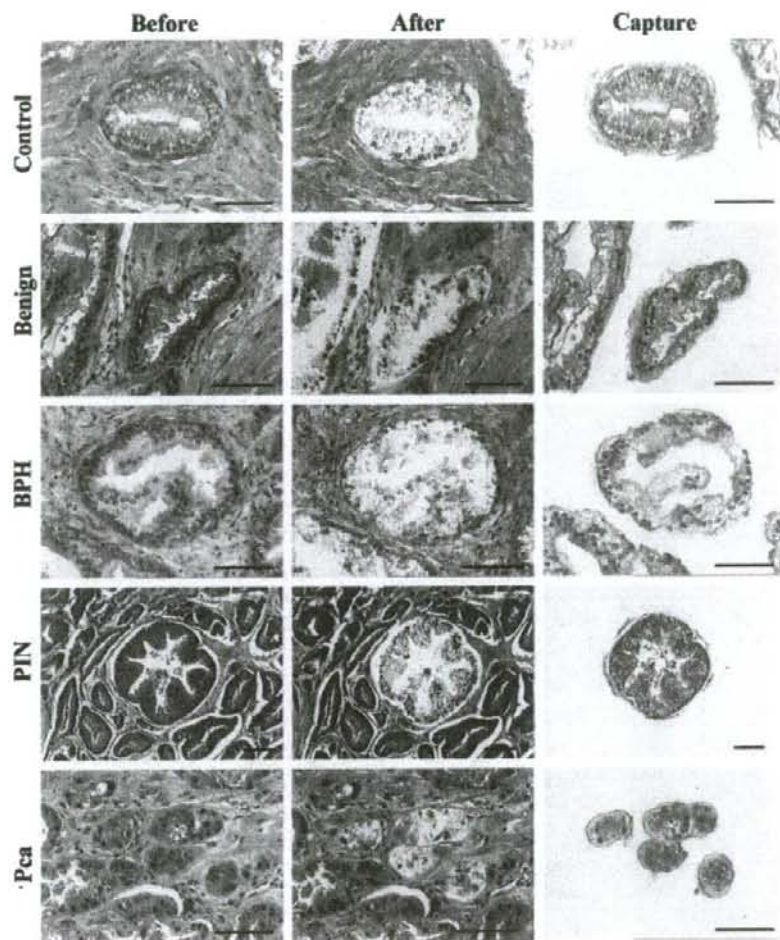
Fig. 1. Representative tissue capture by LCM in early stage prostate cancer tissue and normal control prostate. Methacarn-fixed and paraffin-embedded tissue samples were stained with Cresyl Violet. The Benign, BPH, PIN, and Prostate cancer area were captured from Prostate cancer specimen, while the Control gland was dissected from normal prostate. Scale bars in all panels are 100 μm.

the LPA-degrading enzyme (PAP) all showed distinct expression patterns between the androgen-sensitive LNCaP cells, and the androgen-insensitive PC-3 and Du-145 cells (Fig. 2). While LPA3, AGK, and PAP were predominantly expressed in LNCaP cells, LPA1 and ATX expression were predominant in PC-3 and Du-145 cells. The specificity of the primers used in real-time PCR was also confirmed by conventional PCR, which showed the expected values for each product (data not shown).

Gene Expression Profile in Cancers, HG-PIN, Hyperplastic Glands, Normal Glands, and Surrounding Stroma

Expression levels of all the six LPA-related mRNAs, LPA1, LPA2, LPA3, ATX, AGK, and PAP, were compared between various lesions and control or between epithelial and stromal cells (Fig. 3 and Table II). LPA1 expression in stroma was significantly higher than in the corresponding epithelial component
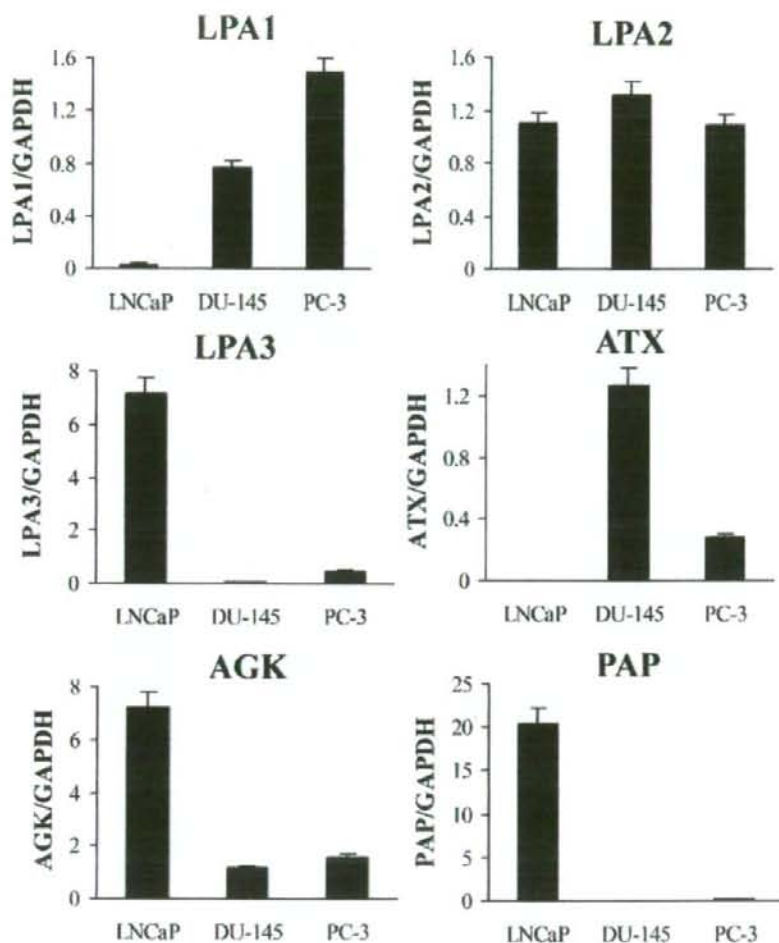
Fig. 2. Distinct expression profiles related to LPA-regulation between LNCaP, DU-145, and PC-3 prostate cancer cells. mRNA levels were determined by quantitative RT-PCR. Values are expressed relative to the expression of GAPDH mRNA. Error bars represent the standard error of the mean for data from two experiments.

in both, cancer foci and HGPIN in hyperplastic glands and control prostate glands (glands in the transition zone prostate of bladder cancer patients). In contrast, LPA2 and LPA3 mRNAs were predominantly expressed in glands than stroma. Further, while a stromal predominance of ATX gene expression was observed, no such difference was found in AGK expression. PAP gene expression was apparently higher in glandular epithelia than its surrounding stroma. LPA1 mRNA expression was significantly decreased in HGPIN and prostate cancer epithelia compared to BPH in the same subject or those in control

prostates. On the other hand, LPA3 expression was significantly elevated in BPH and prostate cancer epithelia. Additionally, mRNA levels of AGK in BPH and its surrounding stroma were respectively higher than those in cancer foci and its associated stroma. PAP expression was significantly increased only in BPH epithelium compared to control prostate samples. As expected, PAP expression was very low in stroma captured from all components. Finally, gene expression profiles of LPA2 and ATX did not changed significantly among different captured components in either epithelium or stroma.

TABLE II. Expression Profiles of LPA-Relating Molecules

Molecules	Glands (G) vs. stroma (S)	Lesions
A: Comparison between glands and stroma		
LPA1	G < S	Ca, PIN, BPH, control
LPA2, 3	G > S	Ca, PIN, BPH, control
ATX	G < S	Ca, PIN, BPH, control
AGK	G = S	Ca, PIN, control
PAP	G ≫ S	Ca, PIN, BPH, control

Molecules	Component	Lesions
B: Comparison between lesions		
LPA1	G	PIN, Ca < BPH, control
LPA3	G	Ca, BPH > control
	S	Ca, BPH > control
AGK	G	BPH > Ca
	S	BPH > Ca

Protein Expression of LPA3, ATX, and AGK in Benign Glands, HG-PIN, and Cancer Foci

LPA 3 protein expression was specifically found in the apical region of excreting cells of benign glands but not in the basal cells. There was little expression in the surrounding stroma (Fig. 4A). On the other hand, LPA3 was strongly expressed in HG-PIN and cancer foci while it was not prominent in the surrounding stroma (Fig. 4B). ATX protein was positively expressed in both cancer cells and the surrounding stroma (Fig. 5A), which is consistent with the early observation on mRNA levels. AGK protein was strongly expressed in HG-PIN and cancer cells while it was very weakly expressed in benign glands as shown in Figure 5B. Stromal expression of AGK was not prominent.

DISCUSSION

In general, the mRNA level of LPA1 was predominant in prostate stroma while those of LPA2 and LPA3 were predominant in epithelia. Immunostaining of LPA3 further support its epithelial predominant expression, although protein localization of LPA1 and LPA2 has not been confirmed. Differences in LPA receptor subtype expression between epithelia and stroma may play a key role in receptor "cross-talk" in the prostate. mRNA level of LPA3 was increased in the cancer foci and BPH as compared to control, while staining intensity of LPA3 protein in cancer epithelia was apparently stronger than that in benign glands. In addition, LPA1 gene expression level was decreased in cancer foci but not in BPH. Another distinct difference between cancer and BPH was AGK gene expression. In BPH epithelia, significantly elevated expression of LPA3, AGK, and PAP were found while LPA1, LPA3,

and AGK expression were increased in the surrounding stroma. These findings suggest that up-regulation of LPA3 may be involved in the development of both prostate cancer and benign hyperplasia although other genes related to LPA-regulation including AGK and PAP may also be involved.

The present results demonstrating that LPA1 gene expression could be detected only in the androgen-independent PC-3 and DU-145 cells, and not in the androgen-sensitive LNCaP cells further confirm and extend earlier reports [32,33]. LPA1 has been shown to mediate the androgen receptor-regulated signal and to promote cell proliferation [19]. It is therefore believed that LPA1 correlates with progression of the prostate cancer to androgen independence rather than the initiation of the disease [14,34]. The down-regulation of LPA1 gene in the HGPIN and early stage prostate cancer foci found in this study further supports the hypothesis that LPA stimulation via LPA1 is not essential in the oncogenesis of prostate cancer. None of the patients in this study were treated with androgen deprivation therapy. Therefore, it remains unclear whether the switching of expression from LPA3 to LPA1 in prostate cancer occurs in response to androgen deprivation or after acquiring androgen independence.

Another interesting finding in this study is that, the stromal cells surrounding benign hyperplastic glands, showed a significant increase in LPA1 expression compared to those surrounding benign glands in the same prostate cancer specimen. We previously found that LPA1 was expressed in both human prostatic stromal cells and epithelial cells and mediated LPA-induced expression of CYP61 which was found to be related to the progression of BPH [22]. The present result further suggests that LPA1 signaling in stroma
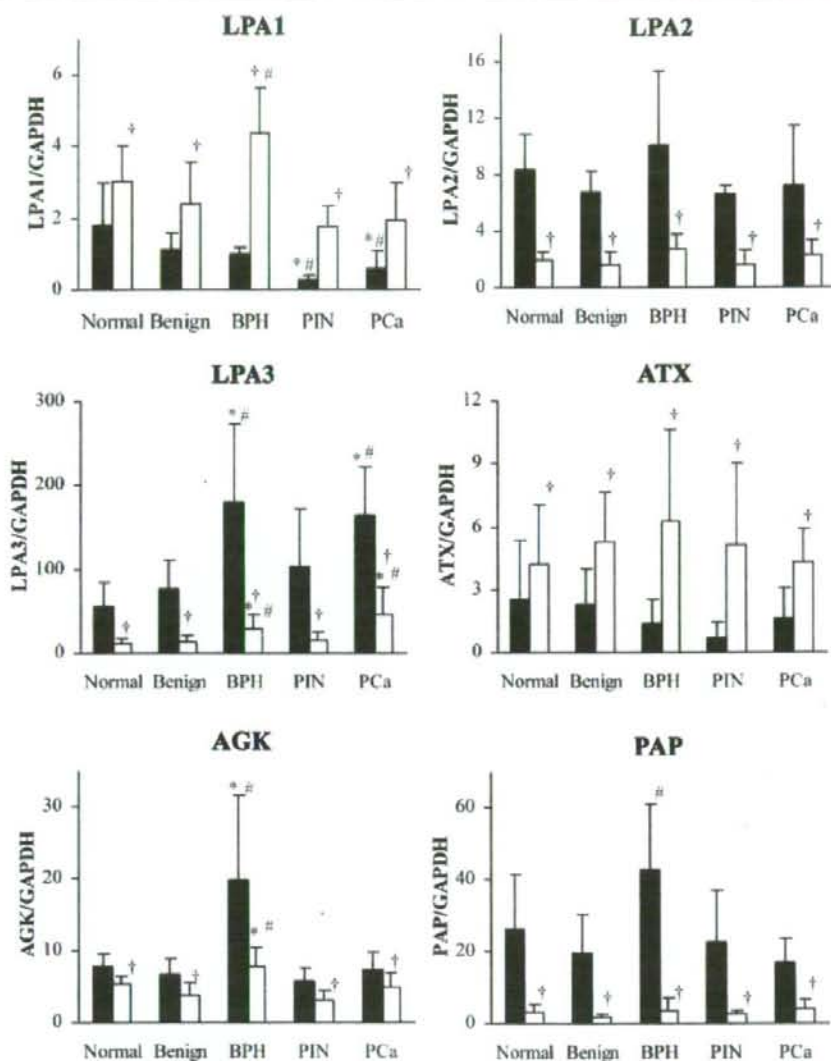
Fig. 3. Divergent expression profile of the genes related to LPA-regulation in the prostate obtained from early stage prostate cancer and in the control prostate obtained from bladder cancer patients. Epithelia (■) and surrounding stroma (□) were microdissected from benign glands (Benign), BPH, high grade PIN (PIN) and prostate cancer (PCa) foci in the prostate harboring prostate cancer, respectively. Benign glands were also microdissected from the normal control prostates (Normal). (*) Comparing to control prostate, (#) comparing to benign gland or surrounding stroma in prostate cancer specimen, (†) comparing to associated epithelia. mRNA levels were determined by quantitative RT-PCR. Values are expressed relative to the expression of GAPDH mRNA (mean ± SD).

rather than epithelium may be critical in BPH development although LPA1 protein expression remains to be analyzed.

In the current study LPA3 gene was highly expressed in the prostatic epithelia rather than the stroma, which was further confirmed at protein levels.

LPA3 plays critical role in normal development such as implantation and embryo spacing [16,35]. Using three lines of Sf9 insect cells that individually expressed LPA receptors, we previously reported that LPA detected in seminal plasma selectively activated LPA3, but not LPA1 or LPA2 [13]. Together, these data suggest that
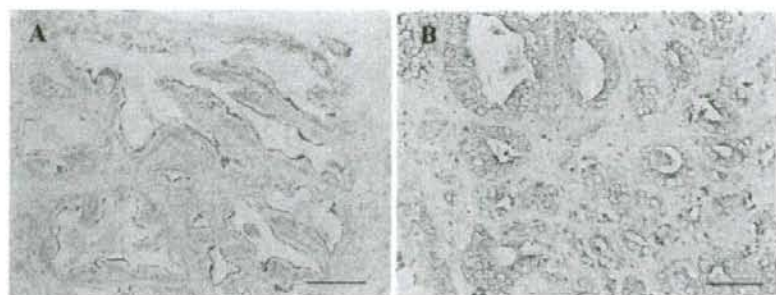
Fig. 4.   Representative immunohistochemical staining of LPA3 in benign gland of prostate (**A**) and cancer foci associated with HG-PIN (**B**). Scale bars are 200 μm.

LPA3-mediated signaling pathways in the prostatic epithelium that is exposed to seminal plasma at its apical surface are important to normal prostate development. Furthermore, it has been shown that expression of constitutively active mutant of Gq, which is coupled by LPA3, promoted LPA-induced activation of nuclear factor-κB (NF-κB) and cell survival in PC-3 cells [18]. It is also interesting that LPA3 expression is maintained in the androgen-sensitive LNCaP cells and not in the androgen-independent PC-3 and Du-145 cells. This may be ascribed to the fact that LNCaP cells mimic the early stage prostate cancer when compared to PC-3 and Du-145 cells [19,36]. However, it remains to be determined whether up-regulation or exogenous gene transfer of LPA3 results in sensitization to androgen deprivation therapy for prostate cancer.

The imbalance of LPA synthesis and metabolism in local microenvironment may affect LPA-regulation in the prostate and consequently contribute to the development of prostate cancer or BPH. However, in the present study, we did not find significant changes in AGK, ATX, and PAP mRNA expression in either cancer or BPH as compared with normal control. On the other hand, preliminary results of our on-going immunohistochemical study on AGK and ATX has

shown that excessive AGK and ATX expression is remarkable in higher grade prostate cancer foci while expression of both protein is weak in HG-PIN and negative in benign glands (unpublished data). It remains to be elucidated whether this discrepancy between mRNA and protein expression as to LPA-producing enzymes can be ascribed to the difference in LPA-degradation enzyme expression.

In summary, the present mRNA and protein analyses suggest that LPA receptors, in particular LPA3, play a pivotal role in the development of both BPH and prostate cancer by mediating LPA-signaling. It remains to be clarified whether change in expression of AGK and ATX, LPA-producing enzymes, is involved in the development or malignant progression of prostate cancer.
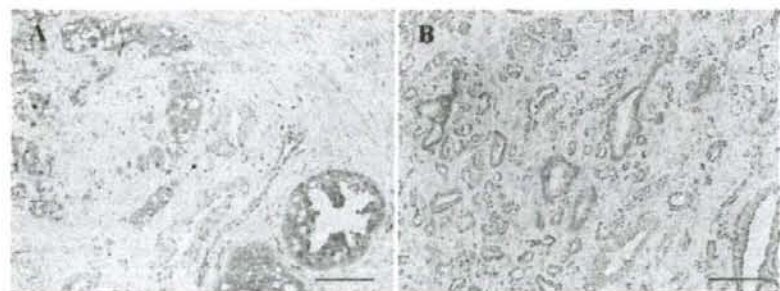
ACKNOWLEDGMENTS

Fig. 5.   Representative immunohistochemical staining of ATX (**A**) and AGK (**B**) in prostate specimen mainly consisting of cancer foci. Both ATX and AGK were positively stained in cancer cells while they were negatively or very weakly stained in benign glands. Scale bars are 200 μm.

of Pharmaceutical Sciences, for kindly providing us with the anti-LPA 3 and anti-AGK monoclonal antibodies. This work was supported in part by a Grant-in-Aid for Scientific Research from the Ministry of Education, Science, Culture and Sports, Japan (18390483).

REFERENCES

1. Grayhack JT, Kozlowski JM. Benign prostatic hyperplasia. In: Gillenwater JY, Grayhack JT, Howards SS, Duckett JM, editors. Adult and pediatric urology, 3rd edition. St. Louis: Mosby; 1996. 1501 p.

2. Grayhack JT, Lee C, Brand W. The effect of testicular irradiation on established BPH in the dog: Evidence of a non-steroidal testicular factor for BPH maintenance. J Urol 1985;134(6):1276–1281.

3. Sutkowski DM, Kasjanski RZ, Sensibar JA, Ney KG, Lim DJ, Kozlowski JM, Lee C, Grayhack JT. Effect of spermatocele fluid on growth of human prostatic cells in culture. J Androl 1993; 14(4):233–239.

4. Juniewicz PE, Berry SJ, Coffey DS, Strandberg JD, Ewing LL. The requirement of the testis in establishing the sensitivity of the canine prostate to develop benign prostatic hyperplasia. J Urol 1994;152(3):996–1001.

5. Grayhack JT, Sensibar JA, Ilio KY, Kasjanski RZ, Kozlowski JM, Lee C. Synergistic action of steroids and spermatocele fluid on in vitro proliferation of prostate stroma. J Urol 1998;159(6):2202–2209.

6. Tigyi G, Parrill AL. Molecular mechanisms of lysophosphatidic acid action. Prog Lipid Res 2003;42(6):498–526.

7. Tokumura A. A family of phospholipid autacoids: Occurrence, metabolism and bioactions. Prog Lipid Res 1995;34(2):151–184.

8. Mills GB, Moolenaar WH. The emerging role of lysophosphatidic acid in cancer. Nat Rev Cancer 2003;3(8):582–591.

9. Yoshida K, Nishida W, Hayashi K, Ohkawa Y, Ogawa A, Aoki J, Arai H, Sobue K. Vascular remodeling induced by naturally occurring unsaturated lysophosphatidic acid in vivo. Circulation 2003;108(14):1746–1752.

10. Sugiura T, Nakane S, Kishimoto S, Waku K, Yoshioka Y, Tokumura A. Lysophosphatidic acid, a growth factor-like lipid, in the saliva. J Lipid Res 2002;43(12):2049–2055.

11. Wang J, Okamoto Y, Morishita J, Tsuboi K, Miyatake A, Ueda N. Functional analysis of the purified anandamide-generating phospholipase D as a member of the metallo-beta-lactamase family. J Biol Chem 2006;281(18):12325–12335.

12. Tokumura A, Miyake M, Nishioka Y, Yamano S, Aono T, Fukuzawa K. Production of lysophosphatidic acids by lysophospholipase D in human follicular fluids of in vitro fertilization patients. Biol Reprod 1999;61(1):195–199.

13. Hama K, Bandoh K, Kakehi Y, Aoki J, Arai H. Lysophosphatidic acid (LPA) receptors are activated differentially by biological fluids: Possible role of LPA-binding proteins in activation of LPA receptors. FEBS Lett 2002;523(1–3):187–192.

14. Kue PF, Daaka Y. Essential role for G proteins in prostate cancer cell growth and signaling. J Urol 2000;164(6):2162–2167.

15. Anliker B, Chun J. Lysophospholipid G protein-coupled receptors. J Biol Chem 2004;279(20):20555–20558.

16. Ye X, Hama K, Contos JJ, Anliker B, Inoue A, Skinner MK, Suzuki H, Amano T, Kennedy G, Arai H, Aoki J, Chun J. LPA3-mediated lysophosphatidic acid signalling in embryo implantation and spacing. Nature 2005;435(7038):104–108.

17. Raj GV, Barki-Harrington L, Kue PF, Daaka Y. Guanosine phosphate binding protein coupled receptors in prostate cancer: A review. J Urol 2002;167(3):1458–1463.

18. Raj GV, Sekula JA, Guo R, Madden JF, Daaka Y. Lysophosphatidic acid promotes survival of androgen-insensitive prostate cancer PC3 cells via activation of NF-kappaB. Prostate 2004; 61(2):105–113.

19. Guo R, Kasbohm EA, Arora P, Sample CJ, Baban B, Sud N, Sivashanmugam P, Moniri NH, Daaka Y. Expression and function of lysophosphatidic acid LPA1 receptor in prostate cancer cells. Endocrinology 2006;147(10):4883–4892.

20. Sivashanmugam P, Tang L, Daaka Y. Interleukin 6 mediates the lysophosphatidic acid-regulated cross-talk between stromal and epithelial prostate cancer cells. J Biol Chem 2004;279(20):21154–21159.

21. Adolfsson PI, Ahlstrand C, Varenhorst E, Svensson SP. Lysophosphatidic acid stimulates proliferation of cultured smooth muscle cells from human BPH tissue: Sildenafil and papaverin generate inhibition. Prostate 2002;51(1):50–58.

22. Sakamoto S, Yokoyama M, Zhang X, Prakash K, Nagao K, Hatanaka T, Getzenberg RH, Kakehi Y. Increased expression of CYR61, an extracellular matrix signaling protein, in human benign prostatic hyperplasia and its regulation by lysophosphatidic acid. Endocrinology 2004;145(6):2929–2940.

23. Tokumura A, Majima E, Kariya Y, Tominaga K, Kogure K, Yasuda K, Fukuzawa K. Identification of human plasma lysophospholipase D, a lysophosphatidic acid-producing enzyme, as autotaxin, a multifunctional phosphodiesterase. J Biol Chem 2002;277(42):39436–39442.

24. Bektas M, Payne SG, Liu H, Goparaju S, Milstien S, Spiegel S. A novel acylglycerol kinase that produces lysophosphatidic acid modulates cross talk with EGFR in prostate cancer cells. J Cell Biol 2005;169(5):801–811.

25. Lin MF, Garcia-Arenas R, Xia XZ, Biela B, Lin FF. The cellular level of prostatic acid phosphatase and the growth of human prostate carcinoma cells. Differentiation 1994;57(2):143–149.

26. Lin MF, Lee MS, Zhou XW, Andressen JC, Meng TC, Johansson SL, West WW, Taylor RJ, Anderson JR, Lin FF. Decreased expression of cellular prostatic acid phosphatase increases tumorigenicity of human prostate cancer cells. J Urol 2001; 166(5):1943–1950.

27. Tanaka M, Kishi Y, Takanezawa Y, Kakehi Y, Aoki J, Arai H. Prostatic acid phosphatase degrades lysophosphatidic acid in seminal plasma. FEBS Lett 2004;571(1–3):197–204.

28. Takagi H, Shibutani M, Kato N, Fujita H, Lee KY, Takigami S, Mitsumori K, Hirose M. Microdissected region-specific gene expression analysis with methacarn-fixed, paraffin-embedded tissues by real-time RT-PCR. J Histochem Cytochem 2004;52(7):903–913.

29. Wu X, Kakehi Y, Zeng Y, Taoka R, Tsunemori H, Inui M. Uroplakin II as a promising marker for molecular diagnosis of nodal metastases from bladder cancer: Comparison with cytokeratin 20. J Urol 2005;174(6):2138–2142.

30. Umezu-Goto M, Kishi Y, Taira A, Hama K, Dohmae N, Takio K, Yamori T, Mills GB, Inoue K, Aoki J, Arai H. Autotaxin has lysophospholipase D activity leading to tumor cell growth and motility by lysophosphatidic acid production. J Cell Biol 2002; 158(2):227–233.

31. Kitayama J, Shida D, Sako A, Hama K, Aoki J, Arai H, Nagawa H. Over-expression of lysophosphatidic acid receptor-2 in human

invasive ductal carcinoma. Breast Cancer Res 2004;6(6):R640–R646.

32. Daaka Y. Mitogenic action of LPA in prostate. Biochim Biophys Acta 2002;1582(1–3):265–269.

33. Im DS, Heise CE, Harding MA, George SR, O'Dowd BF, Theodorescu D, Lynch KR. Molecular cloning and characterization of a lysophosphatidic acid receptor, Edg-7, expressed in prostate. Mol Pharmacol 2000;57(4):753–759.

34. Guo C, Luttrell LM, Price DT. Mitogenic signaling in androgen sensitive and insensitive prostate cancer cell lines. J Urol 2000; 163(3):1027–1032.

35. Bandoh K, Aoki J, Hosono H, Kobayashi S, Kobayashi T, Murakami-Murofushi K, Tsujimoto M, Arai H, Inoue K. Molecular cloning and characterization of a novel human G-protein-coupled receptor, EDG7, for lysophosphatidic acid. J Biol Chem 1999;274(39):27776–27785.

36. Kishi Y, Okudaira S, Tanaka M, Hama K, Shida D, Kitayama J, Yamori T, Aoki J, Fujimaki T, Arai H. Autotaxin is over-expressed in glioblastoma multiforme and contributes to cell motility of glioblastoma by converting lysophosphatidyl-choline to lysophosphatidic acid. J Biol Chem 2006;281(25): 17492–17500.

Epigenetic Modifications of *RASSF1A* Gene through Chromatin Remodeling in Prostate Cancer

Ken Kawamoto,[1] Steven T. Okino,[1] Robert F. Place,[1] Shinji Urakami,[1] Hiroshi Hirata,[1] Nobuyuki Kikuno,[1,2] Toshifumi Kawakami,[1] Yuichiro Tanaka,[1] Deepa Pookot,[1] Zhong Chen,[1] Shahana Majid,[1] Hideki Enokida,[3] Masayuki Nakagawa,[3] and Rajvir Dahiya[1]

Abstract

Purpose: The RAS-association domain family 1, isoform A (*RASSF1A*) gene is shown to be inactivated in prostate cancers. However, the molecular mechanism of silencing of the *RASSF1A* gene is not fully understood. The present study was designed to investigate the mechanisms of inactivation of the *RASSF1A* gene through the analysis of CpG methylation and histone acetylation and H3 methylation associated with the *RASSF1A* promoter region.

Experimental Design: Methylation status of the *RASSF1A* gene was analyzed in 131 samples of prostate cancer, 65 samples of benign prostate hypertrophy (BPH), and human prostate cell lines using methylation-specific PCR. Histone acetylation (acetyl-H3, acetyl-H4) and H3 methylation (dimethyl-H3-K4, dimethyl-H3-K9) status associated with the promoter region in prostate cells were analyzed by chromatin immunoprecipitation (ChIP) assay.

Results: Aberrant methylation was detected in 97 (74.0%) prostate cancer samples and 12 (18.5%) BPH samples. The methylation frequency of *RASSF1A* showed a significant increase with high Gleason sum and high stage. The ChIP assays showed enhancement of histone acetylation and dimethyl-H3-K4 methylation on the unmethylated *RASSF1A* promoter. TSA alone was unable to alter key components of the histone code. However, after 5-aza-2′-deoxy-cytidine treatment, there was a complete reversal of the histone components in the hypermethylated promoter. Levels of acetyl-H3, acetyl-H4, and dimethyl-H3-K4 became more enriched, whereas H3K9me2 levels were severely depleted.

Conclusions: This is the first report suggesting that reduced histone acetylation or H3K4me2 methylation and increased dimethyl-H3-K9 methylation play a critical role in the maintenance of promoter DNA methylation–associated *RASSF1A* gene silencing in prostate cancer.

Prostate cancer is the most commonly diagnosed malignancy and the second leading cause of cancer-related deaths among men in the United States and Europe (1). The incidence of prostate cancer increases with aging (2). Once a tumor has metastasized, the long-term prognosis is poor because no curative therapy is available. Cancer development and metastasis are multistep processes that, among others,

involve the inactivation of tumor suppressor genes. When normal expression levels of these growth-inhibitory proteins are suppressed, uncontrolled cell cycling and growth can result. Identifying such specific molecular changes may contribute to improved diagnosis, clinical management, and outcome prediction of newly diagnosed prostate cancers (3).

Silencing of cancer-associated genes by hypermethylation of CpG islands within the promoter and/or 5′ regions is a common feature of human cancer and is often associated with partial or complete transcriptional block (4). This epigenetic alteration provides an alternative pathway to gene silencing in addition to gene mutation or deletion. Moreover, the finding of promoter methylation of several genes in small biopsies and bodily fluids of cancer patients has proven to be useful as a molecular tool for cancer detection (5, 6).

The RAS-association domain family 1 has seven different isoforms that are produced by alternative splicing and transcription from two different promoters with CpG islands (7, 8). The RAS-association domain family 1, isoform A (*RASSF1A*) gene is a tumor suppressor gene in the RAS pathway that can regulate proliferation, induce apoptosis, and bind to and stabilize microtubules (9). Inactivation of *RASSF1A* is frequently observed in a number of solid tumors and epithelial cancers, including prostate cancer (3, 10–17).

In the present study, we investigated the chromatin changes involved in the inactivation of the *RASSF1A* gene in prostate cancer samples through the analysis of CpG methylation in the promoter regions, histone acetylation (acetyl-H3, acetyl-H4), dimethyl-H3-K4 (H3K4me2), and dimethyl-H3-K9 (H3K9me2) methylation associated with the *RASSF1A* promoter region.

Materials and Methods

Clinical samples. A total of 131 newly diagnosed prostate cancer tissues from radical prostatectomy and 65 pathologically proven benign prostate hypertrophy (BPH) samples from transurethral resection (TUR-P). The pathologic background of the prostate cancer patients included Gleason sum (GS) <7 (75 cases) and GS ≥7 (56 cases); pT2 (85 cases), pT3 (44 cases), and pT4 (2 cases); and preoperative serum PSA <4.0 (18 cases), PSA 4.0-10.0 (63 cases), and PSA >10.0 (50 cases). The median follow-up time was 35.5 months, with a range from 0.7 to 91.4 months. Serum PSA levels after radical prostatectomy was used as a surrogate end point, with a level ≥0.2 ng/mL designated as PSA failure. The median age of prostate cancer and BPH patients was 70 years (49-80 years) and 75 years (54-84 years), respectively. The pathologic findings of prostate cancer samples were decided by the general rule for Clinical and Pathological Studies on Prostate Cancer by the Japanese Urological Association and the Japanese Society of Pathology (18). The routine strategy to diagnose prostate cancer included serum PSA level, transrectal ultrasonography, color Doppler ultrasonography, and MRI, which allowed accurate localization of prostate cancer before radical prostatectomy (19). Each tissue sample was fixed in 10% buffered formalin (pH 7.0) and embedded in paraffin wax. For histologic evaluation, 5-μm-thick sections were used for H&E staining. All of the samples were microscopically dissected and analyzed for methylation (20). In BPH samples, high-grade prostate intraepithelial neoplasia and cancer were ruled out by microscopic analysis.

Cell lines. RWPE-1 and PWR-1E, a nontumorigenic human prostatic epithelial cell line, and the human prostate cancer cell lines LNCaP and PC3 were obtained from the American Type Culture Collection. RWPE-1 and PWR-1E cells were maintained in keratinocyte serum-free medium (Life Technologies) supplemented with 50 μg/mL bovine pituitary extract, 5% L-glutamine, and 5 ng/mL epidermal growth factor. Both prostate cancer cell lines were maintained in RPMI 1640 with L-glutamine and sodium pyruvate. The cells were maintained in a humidified incubator (5% CO_2) at 37°C.

Nucleic acid extraction. Genomic DNA was extracted from cell lines, prostate cancer, and control prostate samples using a QIAamp DNA Mini Kit (Qiagen) after microdissection (20). The concentrations of DNA and RNA were determined spectrophotometrically, and their integrity was assessed by gel electrophoresis.

Methylation analysis. Genomic DNA from all prostate samples (100 ng) was subjected to sodium bisulfite modification using a CpGenome DNA Modification Kit (Intergen Co.). The methylation status of the promoter region of *RASSF1A* was analyzed by methylation-specific PCR (MSP) as described previously (21). The first universal primer set (PAN) covers no CpG sites in either the forward or reverse primer and amplifies a DNA fragment of the promoter region containing a number of CpG sites. Then, a second round of nested MSP or unmethylation-specific PCR (USP) was done using the universal PCR products as templates. Referring to a previous report (22), primer sequences were designed for MSP and USP. The primer sequences and PCR conditions are shown in Table 1. For semiquantitative analysis, a preliminary suitable number of PCR cycles for each MSP and USP were carried out to determine the linear range of the reaction. In each assay, the absence of DNA template served as negative control. CpGenome Universal Methylated DNA (Intergen) was used as a positive control for methylated alleles. The obtained MSP and USP products were analyzed by electrophoresis in 3% agarose gels and stained with ethidium bromide.

Bisulfite DNA sequencing. Bisulfite-modified DNA was amplified using a pair of universal primers. Direct bisulfite DNA sequencing of the PCR products using either forward universal primer or reverse primer was done according to the manufacturer's instructions (Applied Biosystems).

5′-aza-2-deoxycytidine and TSA treatment. Cells were treated with the DNA methyltransferase inhibitor 5-aza-2′-deoxy-cytidine (5-aza-dC; Sigma-Aldrich) at 5 μmol/L for 48 h and/or the histone deacetylase (HDAC) inhibitor trichostatin A (TSA, Upstate Biotechnology) at 300 nmol/L for 24 h. The genomic DNA and total RNA were extracted from the cell lines before and after drug treatment and were used for MSP and reverse transcription-PCR (RT-PCR; TITANIUM One-Step RT-PCR kit, BD Biosciences). The primer sequences (22) and PCR conditions are shown in Table 1.

Chromatin immunoprecipitation assay. Chromatin immunoprecipitation (ChIP) assays were done on cell line DNA using a EZ ChIP (Upstate Biotechnology) and followed the manufacturer's protocols with some modifications. Formaldehyde was added to the cells in a culture dish to a final concentration of 1% and incubated at 37°C for 10 min. The cells were washed in 1 mL of ice-cold PBS with proteinase inhibitors, scraped, and resuspended in 400 μL of SDS lysis buffer. Lysates were sonicated for 10 s nine times on ice and centrifuged at 15,000 rpm for 10 min at 4°C. Supernatants were

Table 1. Primer sequences and PCR conditions

|	Sense primer (5′ → 3′)	Antisense primer (5′ → 3′)	Annealing temperature (°C), PCR cycles	Product size (bp)
MSP primers				
PAN	GGAGGGAAGGAAGGGTAAG	CAACTCAATAAACTCAAACTCCC	54, 40	260
MSP	GGGTTTTGCGAGAGCGCG	GCTAACAAACGCGAACCG	64, 35	169
USP	GGTTTTGTGAGAGTGTGTTTAG	CACTAACAAACACAAACCAAAC	60, 35	169
RT-PCR primers				
RASSF1A	CAGATTGCAAGTTCACCTGCCACTA	GATGAAGCCTGTGTAAGAACCGTCCT	60, 33	242
GAPDH	GAGTCAACGGATTTGGTCGT	TGGAATCATATTGGAACATGTAAA	60, 32	135
ChIP primers				
1	GATCACGGTCCAGCCTCTGC	CTCGAGCCTTCACTTGGGGT	60, 32	109
2	GCTTCAGCAAACCGGACCAGG	CCGGACGGCCACAACGA	60, 32	134
3	TGGGGTGTGAGGAGGGGACGA	AGAGCCGCGCAATGGA	60, 32	124
4	GTTTCCATTGCGCGGCTCT	CTGGCTTTGGGCGCTAGCAAG	60, 32	124
GAPDH	TACTAGCGGTTTTACGGGCG	TCGAACAGGAGGAGCAGAGAGCGA	60, 32	166
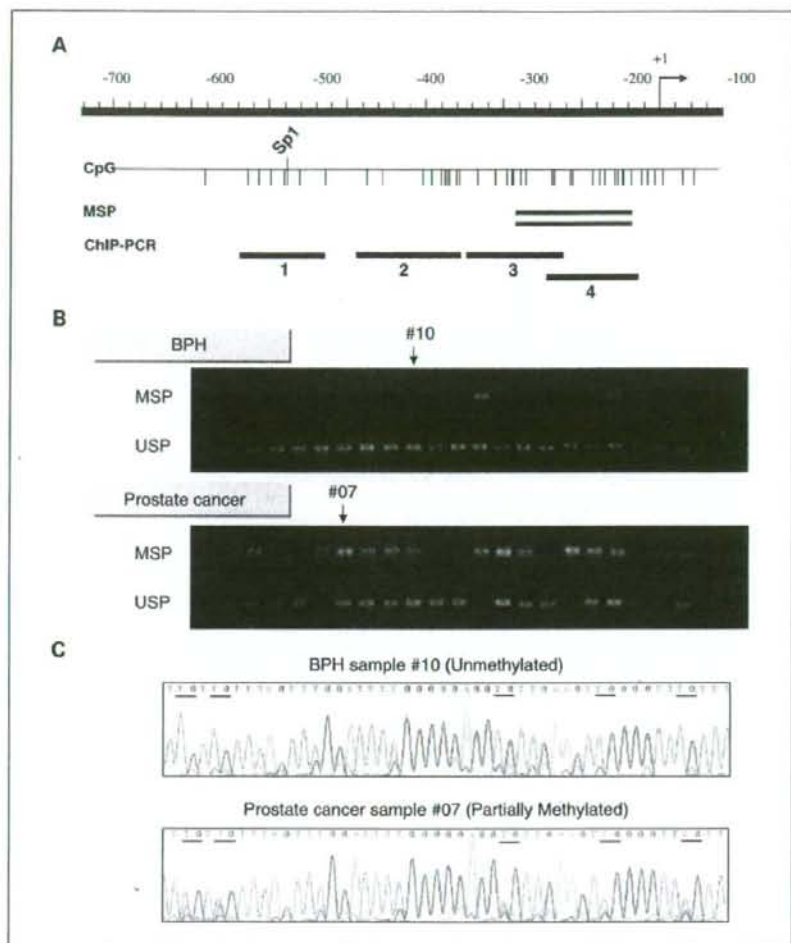
Fig. 1. *A,* schematic representation of the promoter region of the human *RASSF1A* gene. Vertical lines, location of CpG dinucleotides; arrow, approximate position of the transcription start site. Doubled horizontal line, region examined by MSP. Four horizontal bars, location of the DNA fragments amplified by PCR done on the DNA recovered from ChIP assay. *B,* typical MSP results in BPH and prostate cancer samples are shown. Methylated bands were detected in 97 (74.0%) of the prostate cancer samples and in only 12 (18.5%) of the BPH samples. *C,* bisulfite DNA sequencing of unmethylated (*top*) and partially methylated (*bottom*) samples. In unmethylated samples, every CpG site was unmethylated. In partially methylated samples, there was a "T" peak along with a "C" peak at the CpG sites. Bars under the sequence, CpG sites. The results of the bisulfite DNA sequencing were consistent with those obtained by MSP.

loaded on 1% agarose gels and determined to have reduced DNA lengths between 200 and 1,000 bp. The sonicated samples were precleaned with salmon sperm DNA/protein A agarose beads (Upstate Biotechnology). The soluble chromatin fraction was collected, and 8 μL of antibody for acetyl-H3, acetyl-H4, dimethyl-H3-K4 (H3K4me2), or 12 μL of antibody for dimethyl-H3-K9 (H3K9me2), or no antibody, was added and incubated overnight with rotation (23). All antibodies were purchased from Upstate Biotechnology. After rotation, chromatin-antibody complexes were collected using salmon sperm DNA/protein A agarose beads and washed according to the manufacturer's protocol. Immunoprecipitated DNA was recovered using a QIAquick PCR Purification Kit (Qiagen) and analyzed by PCR. We used previously reported (23, 24) primers designed to separately amplify four regions in the *RASSF1A* promoter area (Fig. 1A). The primer pairs used for ChIP assays are shown in Table 1. One additional primer set was used to amplify a 166-bp fragment of the glyceraldehyde-3-phosphate dehydrogenase (*GAPDH*) gene as an internal control. Each PCR reaction was initially set up using different amounts of ChIP sample with varying PCR cycle numbers, and we selected the final PCR conditions accordingly. PCR products were analyzed on 3.0% agarose gels and visualized by UV illumination. Densitometric analysis

of the observed bands was done using ImageJ software.[4] Relative enrichment was calculated by taking the ratio between the net intensity of the *RASSF1A* PCR product from each primer set and the net intensity of the *GAPDH* PCR product for the bound sample and dividing this by the same ratio calculated for the input sample (25). The value of each point was calculated as the average from two independent ChIP experiments and a total of four independent PCR analyses.

Statistical analysis. The relationship between clinicopathologic findings and methylation status of the *RASSF1A* gene was done using the χ^2 test and Fisher's exact test. For each clinicopathologic finding, the association with PSA failure-free probability was determined using Kaplan-Meier curves, and a log-rank test was used to determine significance. *P* values of <0.05 were regarded as statistically significant. All statistical analyses were done using StatView version 5.0 for Windows.
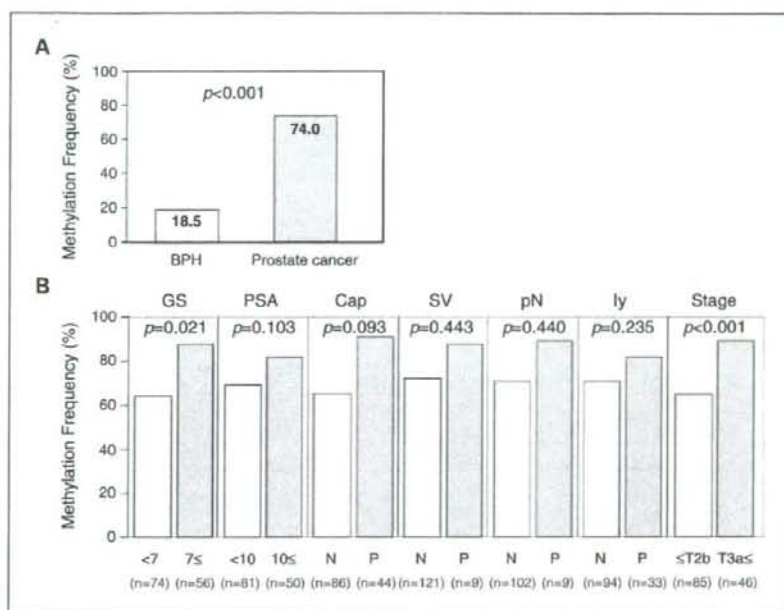
---

[4] http://rsb.info.nih.gov/ij

Fig. 2. Correlation of clinicopathologic features with methylation frequency of the *RASSF1A* promoter. *A*, the difference in the frequency of *RASSF1A* promoter methylation was significant between prostate cancer and BPH samples. *B*, there was significant correlation between methylation frequency of *RASSF1A* and high GS or clinical stage. Methylation frequency of *RASSF1A* increased with higher GS and high stage. The total number of patients was 131, but some patients were lacking clinicopathologic findings, and then data were not included. Cap, capsular invasion; SV, seminal vesicle involvement; pN, lymph node invasion; ly, lymphatic vessel invasion. N and P, negative and positive, respectively.

Results

Methylation status of RASSF1A gene. Typical examples of MSP and USP bands obtained during methylation analysis of the *RASSF1A* promoter are shown in Fig. 1B. To confirm the methylation status of the *RASSF1A* promoter, bisulfite-modified DNA was amplified and sequenced. Typical bisulfite-modified DNA sequencing of prostate cancer and BPH samples are shown in Fig. 1C. In BPH samples, most CpG sites were not methylated, whereas in prostate cancer samples, most CpG sites were methylated in the promoter region. In the total group of prostate cancer and BPH, there was no correlation between age and methylation. In the 131 prostate cancer samples, positive *RASSF1A* methylation was detected in 97
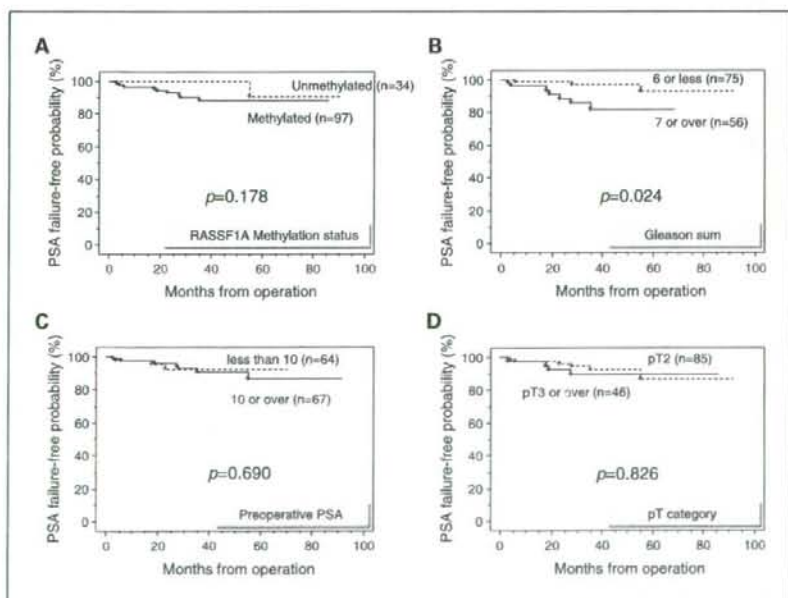

Fig. 3. Kaplan-Meier PSA failure-free survival curves of prostate cancer patients after radical prostatectomy, grouped according to the evaluated variables. *A*, methylation frequency of *RASSF1A*; *B*, GS; *C*, preoperative PSA; *D*, pT category. Follow-up ranged from 0.7 to 91.4 mo, with a median of 35.5 mo.

Fig. 4. *A*, RT-PCR analysis of *RASSF1A* expression in a normal prostatic epithelial cell lines and two prostate cancer cell lines. The mRNA transcript of *RASSF1A* was significantly increased after 5-aza-dC treatment alone or with a combination of 5-aza-dC and TSA in PWR-1E and the two cancer cell lines. In contrast, TSA treatment failed to re-express the *RASSF1A* gene in these cell lines. *GAPDH* expression served as a loading control. *B*, MSP analysis of *RASSF1A*. MSP analysis showed partial demethylation of the *RASSF1A* promoter region after 5-aza-dC treatment in prostate cancer cell lines. M, reactions specific for methylated DNA; U, reactions specific for unmethylated DNA.
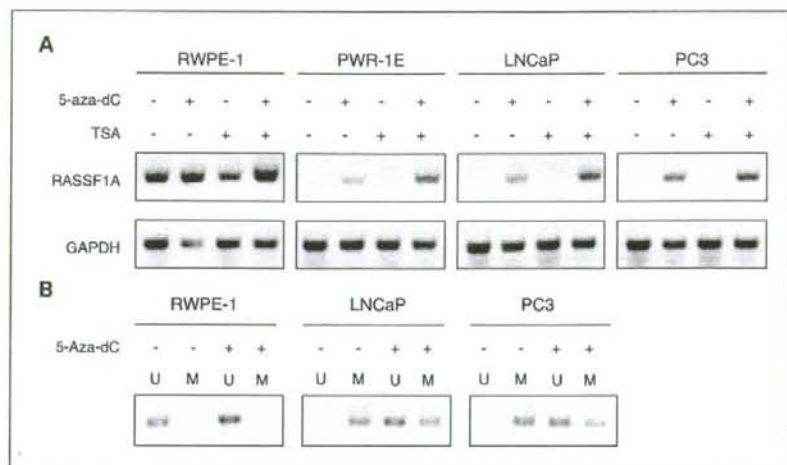
samples (74.0%). On the other hand, in 65 BPH samples, positive *RASSF1A* methylation was detected in 12 samples (18.5%). The difference in the frequency of *RASSF1A* promoter methylation was significant between prostate cancer and BPH samples ($P < 0.001$; Fig. 2A). The methylation frequency of *RASSF1A* showed a significant increase with high GS (63% in GS <7, and 88% in GS ≥7; $P = 0.002$; Fig. 2B) and clinical stage (65% in stage ≤T2b and 91% in stage ≥T3a; $P < 0.001$; Fig. 2B). Although there was a tendency toward increased *RASSF1A* promoter methylation, there was no significant association with high PSA or other pathologic categories (Fig. 2B). PSA failure-free probability was analyzed as disease-free survival, with PSA failure occurring in 10 patients (7.6%). Of the clinicopathologic features considered, only GS was significantly associated with poor outcome ($P = 0.022$; Fig. 3B).

Effects of 5-aza-dC and TSA on RASSF1A gene expression in prostate cancer cells. To clarify the role of epigenetic suppression of the *RASSF1A* gene, we treated prostate cancer cell lines with 5-aza-dC and TSA. At baseline, expression of the *RASSF1A* mRNA transcript was detected in the normal prostate cell line (RWPE-1), but was negative in PWR-1E and prostate cancer cell lines (LNCaP and PC3). With TSA treatment, *RASSF1A* re-expression was not detected in prostate cancer cell lines. However, the expression level was significantly increased in both prostate cancer cell lines after treatment with the demethylating agent 5-aza-dC or combined treatment with azaC and TSA (Fig. 4A). To determine the effects of the demethylating agent, we examined the methylation status in LNCaP and PC3 cells after 5-aza-dC treatment. In both cell lines, partial demethylation was detected by MSP (Fig. 4B).

ChIP assay. The association of *RASSF1A* promoter methylation and gene silencing in relation to chromatin remodeling has not been reported previously in prostate cancer. To establish this functional link, we examined local histone acetylation and H3 methylation in the chromatin associated with the *RASSF1A* promoter region using a ChIP assay. The histone-associated DNAs, immunoprecipitated with antibodies against acetyl-H3, acetyl-H4, H3K4me2, or H3K9me2, were individually amplified with four primer sets covering the

RASSF1A promoter region (Fig. 1A). The results in Fig. 5 show marked differences in the levels of histone acetylation and H3 methylation. Enhancement of histone acetylation and H3K4me2 methylation was observed in RWPE-1 cells, in which the *RASSF1A* promoter is unmethylated and transcriptionally active; however, there was no acetylation or methylation of these same sites in the hypermethylated, transcriptionally silenced promoters (PWR-1E, LNCaP, and PC3). In contrast, H3K9me2 was enriched along the entire hypermethylated and transcriptionally inactive promoters.

To investigate the effect of DNA methyltransferase inhibitor and HDAC-I in the histone modifications of *RASSF1A* promoter, we treated LNCaP cells with 5-aza-dC and/or TSA (Fig. 6A and B). The ChIP assays revealed that TSA treatment alone did not induce any alteration of histone modification. These data show that in addition to being unable to reactivate expression of a hypermethylated, silenced *RASSF1A* gene, TSA alone was unable to evoke obvious change in key parameters of the histone code in the *RASSF1A* promoter (25). In contrast, we observed a complete reversal of the histone modifications after 5-aza-dC treatment alone or the combination of 5-aza-dC and TSA. Acetyl-H3, acetyl-H4, and H3K4me2 levels were higher, whereas H3K9me2 levels were lower in the promoter region.

Discussion

Transcriptional gene silencing by hypermethylation of CpG islands in the promoter region is becoming recognized as a common mechanism for the inactivation of tumor suppressor genes in human malignancies (26–28). In recent years, the list of tumor suppressor genes that are inactivated by epigenetic events rather than classic mutation/deletion events has been growing (7). Unlike mutational inactivation, methylation is reversible, and demethylating agents and inhibitors of HDACs are being used in clinical trails (7).

DNA methylation is an important mechanism in prostate cancer and is involved in the inactivation of various essential genes such as E-cadherin (29), MDR1 (30), and glutathione S-transferase P1 (31). In this study, we found that the *RASSF1A*

gene was methylated in 74% of prostate cancer cases examined. Liu et al. (15) has also reported that *RASSF1A* methylation was frequently observed in prostate cancer (71%). *RASSF1A* functions as a tumor suppressor gene through several distinct pathways, including microtubule stability (32, 33) and cell cycle regulation (8, 16, 34). The *RASSF1A* gene has several isoforms, including *RASSF1A* and *RASSF1C* that are transcribed from two different promoters containing CpG islands (10, 11). Selective promoter methylation of the *RASSF1A* promoter, but not RASSF1C, is frequent in many cancers, including lung, breast, ovarian, and renal cell carcinomas (10–13). In prostate cancer, inactivation of the *RASSF1A* gene was reported to be related to carcinogenesis, and Maruyama et al. (3) described a significant correlation between methylation status, GS, PSA levels, and stage. The results of the present study also showed that *RASSF1A* promoter methylation was associated with high GS and clinical stage. Currently, Rosenbaum et al. (35) reported that the methylation status of selected genes (GSTPI, APC) in prostate cancer specimens may be predictive for time to recurrence in patients undergoing prostatectomy. We also analyzed PSA failure-free probability as disease-free survival. Of the clinicopathologic features considered, only GS was significantly associated with poor outcome.

The mechanisms of *RASSF1A* epigenetic change in relation to prostate tumorigenesis, especially chromatin structural changes during the silencing of the genes, are not known. Thus, we examined the molecular mechanisms of inactivation of the *RASSF1A* gene by analysis of chromatin remodeling such as CpG methylation in the promoter regions, histone acetylation (acetyl-H3, acetyl-H4), dimethyl-H3-K4 (H3K4me2) and di-methyl-H3-K9 (H3K9me2) methylation associated with the *RASSF1A* promoter region. Histone acetylation and H3K4me2 methylation were increased in the unmethylated RWPE-1 *RASSF1A* promoter; however, there was no acetylation or methylation of these same sites in the hypermethylated LNCaP and PC3 promoter. In contrast, H3K9me2 was enriched along the entire hypermethylated and transcriptionally inactive promoter in LNCaP and PC3 cells. Similar results has been reported in breast cancer (23, 24). These results support the idea that DNA methylation-mediated gene silencing is closely linked with repressive histone modifications at the gene promoter in cancer cells (23, 25, 36).

In this study, we also investigated the effect of a DNA methyltransferase inhibitor (5-aza-dC) and/or a HDAC-inhibitor (TSA) on chromatin remodeling. We treated LNCaP cells with TSA alone, but there was no change in histone acetylation and H3
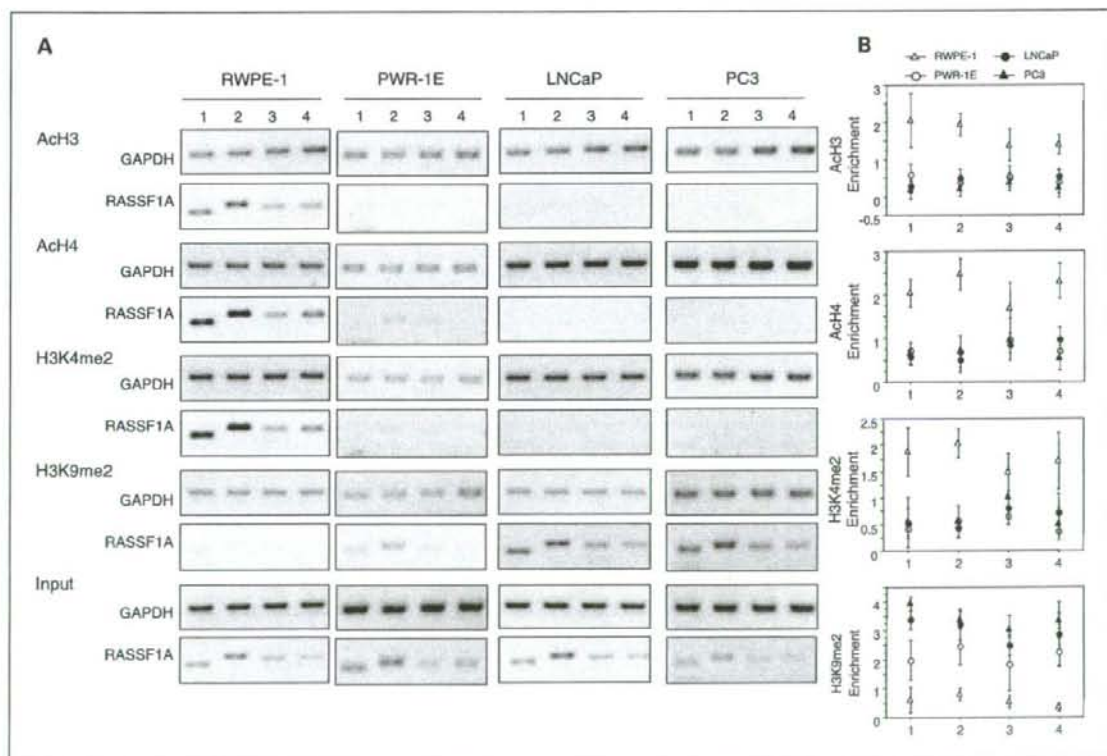

Fig. 5. ChIP assays of the *RASSF1A* CpG island. Chromatin DNA was immunoprecipitated with antibodies specific for acetyl-H3, acetyl-H4, dimethyl-H3-K4 (H3K4me2), and dimethyl-H3-K9 (H3K9me2), respectively. DNA fragments corresponding to *RASSF1A* promoter regions 1, 2, 3, and 4 (see Fig. 1A) were amplified by PCR. Enhancement of histone acetylation and H3K4me2 methylation was observed in the RWPE-1 promoter. However, there was no acetylation or methylation of these same sites in PWR-1E, LNCaP, and PC3 cells. In contrast, H3K9me2 was enriched in these cell lines. *A*, PCR analyses of ChIP assay on RWPE-1, PWR-1E, LNCaP, and PC3 cells in the four promoter regions. *B*, points, enrichment data calculated from the corresponding DNA fragments amplified by PCR; bars SD.

133

Fig. 6. Effects of 5-aza-dC and TSA on the histone modifications of the *RASSF1A* promoter. ChIP assays were done on LNCaP cells after treatment with 5 μmol/L 5-aza-dC for 48 h and/or 300 nmol/L TSA for 24 h. TSA treatment alone did not induce any alteration of histone modification. In contrast, complete reversal of the histone modifications were observed after 5-aza-dC treatment alone or the combination of 5-aza-dC and TSA. Acetyl-H3, acetyl-H4, and H3K4me2 levels were higher, whereas H3K9me2 levels were lower in this region of the promoter. *A*, PCR analyses of ChIP assays. *B*, points, enrichment data calculated from the corresponding DNA fragments amplified by PCR; bars, SD.

methylation. In contrast, after 5-aza-dC treatment alone or a combination of 5-aza-dC and TSA, there was increased accumulation of acetylated histones and H3K4me2 methylation concomitant with reactivation of the methylated *RASSF1A* promoter. These results favor the idea that DNA methylation is more important compared with histone deacetylation in maintaining a silent state at hypermethylated promoters because 5-aza-dC can reactivate genes silenced with aberrant promoter hypermethylation, but TSA alone did not reactivate these genes (37). This change in histone modification upon inhibition of DNA methyltransferase suggests that in prostate cancer cells, DNA hypermethylation, or another activity mediated by DNA methyl-

transferase, may also be essential for maintaining repressive histone modifications at gene promoters silenced by aberrant DNA hypermethylation (25). Furthermore, the observation that 5-aza-dC can both reactivate expression of the silenced *RASSF1A* gene and completely reverse key histone modifications surrounding the gene promoter strengthens the idea that interdependence exists between these two events.

In conclusion, this is the first report suggesting that chromatin remodeling, such as reduced histone acetylation and H3K4me2 methylation, and increased H3K9me2 methylation play a critical role in the maintenance of promoter DNA methylation-associated gene silencing in prostate cancer.

References

1. Jemal A, Ward E, Hao Y, Thun M. Trends in the leading causes of death in the United States, 1970–2002. JAMA 2005;294:1255–9.
2. Perry AS, Foley R, Woodson K, Lawler M. The emerging roles of DNA methylation in the clinical management of prostate cancer. Endocr Relat Cancer 2006; 13:357–77.
3. Maruyama R, Toyooka S, Toyooka KO, et al. Aberrant promoter methylation profile of prostate cancers and its relationship to clinicopathological features. Clin Cancer Res 2002;8:514–9.
4. Esteller M. CpG island hypermethylation and tumor suppressor genes: a booming present, a brighter future. Oncogene 2002;21:5427–40.
5. Jeronimo C, Henrique R, Hoque MO, et al. A quantitative promoter methylation profile of prostate cancer. Clin Cancer Res 2004;10:8472–8.
6. Sidransky D. Emerging molecular markers of cancer. Nat Rev Cancer 2002;2:210–9.
7. Agathanggelou A, Cooper WN, Latif F. Role of the Ras-association domain family 1 tumor

suppressor gene in human cancers. Cancer Res 2005; 65:3497–508.

8. Pfeifer GP, Dammann R. Methylation of the tumor suppressor gene RASSF1A in human tumors. Biochemistry (Mosc) 2005;70:576–83.

9. Liu L, Broaddus RR, Yao JC, et al. Epigenetic alterations in neuroendocrine tumors: methylation of RAS-association domain family 1, isoform A and p16 genes are associated with metastasis. Mod Pathol 2005;18: 1632–40.

10. Burbee DG, Forgacs E, Zochbauer-Muller S, et al. Epigenetic inactivation of RASSF1A in lung and breast cancers and malignant phenotype suppression. J Natl Cancer Inst 2001;93:691–9.

11. Dammann R, Li C, Yoon JH, Chin PL, Bates S, Pfeifer GP. Epigenetic inactivation of a RAS association domain family protein from the lung tumour suppressor locus 3p21.3. Nat Genet 2000;25:315–9.

12. Agathanggelou A, Honorio S, Macartney DP, et al. Methylation associated inactivation of RASSF1A from region 3p21.3 in lung, breast and ovarian tumours. Oncogene 2001;20:1509–18.

13. Dreijerink K, Braga E, Kuzmin I, et al. The candidate tumor suppressor gene, RASSF1A, from human chromosome 3p21.3 is involved in kidney tumorigenesis. Proc Natl Acad Sci U S A 2001;98:7504–9.

14. Yegnasubramanian S, Kowalski J, Gonzalgo ML, et al. Hypermethylation of CpG islands in primary and metastatic human prostate cancer. Cancer Res 2004; 64:1975–86.

15. Liu L, Yoon JH, Dammann R, Pfeifer GP. Frequent hypermethylation of the RASSF1A gene in prostate cancer. Oncogene 2002;21:6835–40.

16. Dammann R, Schagdarsurengin U, Seidel C, et al. The tumor suppressor RASSF1A in human carcinogenesis: an update. Histol Histopathol 2005;20: 645–63.

17. Bastian PJ, Ellinger J, Wellmann A, et al. Diagnostic and prognostic information in prostate cancer with the help of a small set of hypermethylated gene loci. Clin Cancer Res 2005;11:4097–106.

18. The Japanese Urological Association and Japanese Society of Pathology. General rules for clinical and pathological studies on prostate cancer. 2nd ed. Tokyo (Japan): Kanahara-shuppan Co.; 1992.

19. Shigeno K, Igawa M, Shiina H, Kishi H, Urakami S. Transrectal colour Doppler ultrasonography for quantifying angiogenesis in prostate cancer. BJU Int 2003; 91:223–6.

20. Dahiya R, Lee C, McCarville J, Hu W, Kaur G, Deng G. High frequency of genetic instability of microsatellites in human prostatic adenocarcinoma. Int J Cancer 1997;72:762–7.

21. Herman JG, Graff JR, Myohanen S, Nelkin BD, Baylin SB. Methylation-specific PCR: a novel PCR assay for methylation status of CpG islands. Proc Natl Acad Sci U S A 1996;93:9821–6.

22. Lo KW, Kwong J, Hui AB, et al. High frequency of promoter hypermethylation of RASSF1A in nasopharyngeal carcinoma. Cancer Res 2001;61:3877–81.

23. Yan PS, Shi H, Rahmatpanah F, et al. Differential distribution of DNA methylation within the RASSF1A CpG island in breast cancer. Cancer Res 2003;63: 6178–86.

24. Strunnikova M, Schagdarsurengin U, Kehlen A, Garbe JC, Stampfer MR, Dammann R. Chromatin inactivation precedes de novo DNA methylation during the progressive epigenetic silencing of the RASSF1A promoter. Mol Cell Biol 2005;25:3923–33.

25. Fahrner JA, Eguchi S, Herman JG, Baylin SB. Dependence of histone modifications and gene expression on DNA hypermethylation in cancer. Cancer Res 2002;62:7213–8.

26. Jones PA, Laird PW. Cancer epigenetics comes of age. Nat Genet 1999;21:163–7.

27. Baylin SB. Herman JG. DNA hypermethylation in tumorigenesis: epigenetics joins genetics. Trends Genet 2000;16:168–74.

28. Kawaguchi K, Oda Y, Saito T, et al. DNA hypermethylation status of multiple genes in soft tissue sarcomas. Mod Pathol 2006;19:106–14.

29. Li LC, Zhao H, Nakajima K, et al. Methylation of the E-cadherin gene promoter correlates with progression of prostate cancer. J Urol 2001;166:705–9.

30. Enokida H, Shiina H, Igawa M, et al. CpG hypermethylation of MDR1 gene contributes to the pathogenesis and progression of human prostate cancer. Cancer Res 2004;64:5956–62.

31. Enokida H, Shiina H, Urakami S, et al. Ethnic group-related differences in CpG hypermethylation of the GSTP1 gene promoter among African-American, Caucasian and Asian patients with prostate cancer. Int J Cancer 2005;116:174–81.

32. Mathe E. RASSF1A, the new guardian of mitosis. Nat Genet 2004;36:117–8.

33. Jackson PK. Linking tumor suppression, DNA damage and the anaphase-promoting complex. Trends Cell Biol 2004;14:331–4.

34. Shivakumar L, Minna J, Sakamaki T, Pestell R, White MA. The RASSF1A tumor suppressor blocks cell cycle progression and inhibits cyclin D1 accumulation. Mol Cell Biol 2002;22:4309–18.

35. Rosenbaum E, Hoque MO, Cohen Y, et al. Promoter hypermethylation as an independent prognostic factor for relapse in patients with prostate cancer following radical prostatectomy. Clin Cancer Res 2005;11: 8321–5.

36. Jones PA, Baylin SB. The fundamental role of epigenetic events in cancer. Nat Rev Genet 2002;3: 415–28.

37. Cameron EE, Bachman KE, Myohanen S, Herman JG, Baylin SB. Synergy of demethylation and histone deacetylase inhibition in the re-expression of genes silenced in cancer. Nat Genet 1999;21:103–7.

135

Fate of Seminal Vesicles and Prostate After Medical Castration: How Long Is the Optimal Duration of Neoadjuvant Treatment for Prostate Cancer Before Radiation?

Ryoji Furuya, Shin-ichi Hisasue, Seiji Furuya, Nobuhito Saitoh, Hiroshi Ogura, Satoshi Takahashi, and Taiji Tsukamoto

OBJECTIVES   To clarify the morphological alteration of prostate and seminal vesicles (SV) quantitatively after testosterone ablation, we investigated the prostate volume (PV) and the SV volume (SVV) using transrectal ultrasonography.

METHODS   Between July 2002 and October 2004, we prospectively investigated 29 prostate cancer patients. The medical castration group included 21 patients (42 SV and 21 prostate; median Gleason sum, 74 years) who were diagnosed as having T1b to T3aN0M0 prostate cancer and underwent androgen ablation with a luteinizing hormone-releasing hormone (LH-RH) analogue and chlormadinone acetate. As normal controls, 8 patients (16 SV and 8 prostate; median age, 68.5 years) with T1aN0M0 prostate cancer without any other additional treatment were enrolled in this study. We measured both PV and SVV in these groups with transrectal ultrasonography.

RESULTS   Both PV and SVV significantly decreased in the medical castration group (PV: 28.4 ± 9.3 mL to 17.0 ± 5.3 mL, SVV: 3.5 ± 1.8 mL to 1.9 ± 1.0 mL; median, 6 months), whereas those in the control group were maintained (PV: 16.6 ± 5.7 mL to 16.5 ± 5.3 mL, SVV: 2.5 ± 1.0 mL to 2.6 ± 1.6 mL; median, 12 months). In longitudinal assessment, mean PSA, PV, and SVV were significantly reduced gradually up to 12 months after medical castration.

CONCLUSIONS   Not only PV but also SVV was significantly reduced after medical castration. Moreover, size reduction continued up to 12 months in SV, with especially marked reduction seen through the first 6 months. These results demonstrated that optimum duration for androgen ablation before radiotherapy is at least 6 months, and up to 12 months for the maximum effect.   UROLOGY 72: 417–421, 2008. © 2008 Elsevier Inc.

I t has been established that the size of male reproductive organs such as the testis, seminal vesicles (SV), and prostate depends on the androgen level, which was quantitatively analyzed in animal models.[1-4] However, there are few reports regarding such an analysis for humans.[5] Furthermore, to our knowledge, there has been no report on either longitudinal or quantitative analysis regarding volume reduction of the human prostate and SV after androgen ablation.

Radiotherapy is known to be highly effective for organ-confined or locally advanced prostate cancer.[6,7] However, it has also been suggested that for some cases radiotherapy alone is not sufficient.[8] Volume reduction of the prostate and SV has a considerable effect on the treatment strategy to enhance the efficacy and the safety

of radiotherapy for T2 or T3 prostate cancer.[9] It has not been established, however, how long patients should undergo hormonal treatment before radiation from the aspect of the morphological changes of the prostate and SV. Thus, to optimize the radiotherapy strategy for prostate cancer, we investigated the morphological alterations of both SV volume (SVV) and prostate volume (PV) quantitatively after medical castration.

MATERIAL AND METHODS

Between July 2002 and October 2004, 29 prostate cancer patients were enrolled and investigated prospectively. The medical castration group included 21 patients (42 SV and 21 prostate), who were diagnosed as having T1b to T3aN0M0 prostate cancer according to 1997 TNM classification by prostate biopsy (17 patients) or transurethral resection of the prostate (TURP) (4 patients), and underwent medical castration with a luteinizing hormone-releasing hormone (LH-RH) analogue (leuprorelin acetate 3.75 mg every 4 weeks) and chlormadinone acetate (100 mg every day). As normal controls, 8 patients (16 SV

Table 1. Patients' characteristics

	Medical Castration Group	Controls	P-Value*
No. of patients (No. of SV)	21 (42)	8 (16)	
Median age (yr [range])	74 (67–85)	68 (64–79)	0.06
Median serum PSA (ng/mL)	12.7 (4.2–43.7)	1.0 (0.2–3.1)	<0.01
Median follow-up (mo [range])	6 (3–16)	12 (3–19)	0.03
Clinical stage (No.)	T1a (4), T1c (6)	T1a (8)	
	T2a (5), T2b (1)		
	T3a (5)		
Median Gleason sum (range)	7 (5–10)	5 (3–6)	<0.01

PSA, prostate-specific antigen; *SV*, seminal vesicles.

and 8 prostate) with T1aN0M0 prostate cancer after TURP were enrolled in this study. They were observed in a watchful waiting manner without any other additional treatments. Serum prostate-specific antigen (PSA) was within the normal range and there were no abnormal palpable lesions within the prostate on digital rectal examination. Table 1 lists the patients' characteristics. There were significant differences in PSA level, follow-up period and Gleason sum.

The study protocol was approved by the ethics committee and Institutional Review Board of the Kitami Medical Association. All patients were informed about the risks and benefits, and agreed to participate by written informed consent.

Transrectal Ultrasonography (TRUS) Imaging Study
We performed TRUS imaging studies using an ALOKA SSD-5000 ultrasound apparatus (ALOKA, Ltd., Tokyo, Japan) with a biplane high-resolution 5.0- to 7.5-MHz transrectal transducer. Prostate volume (in milliters) was determined using the formula: 0.523 × anterior-posterior diameter (cm) × transverse diameter (cm) × longitudinal diameter (cm). The maximum anterior-posterior diameters of both right and left SV were measured in the transverse view. The maximum lateral diameter of the SV was measured in the longitudinal view by handling the probe parallel to the lateral diameter (Fig. 1). We determined SVV using the formula: 0.523 × (anterior-posterior diameter [cm])² × lateral diameter (cm). The anterior-posterior diameter of SV and SVV were chosen to be evaluation items for SV, and we usually expressed the value as mean of both SV. Every TRUS examination was performed after at least a 3-day abstinence period just in case, although it was already reported that the seminal vesicle size did not change after ejaculation.[10]

Cross-sectional Study
We cross-sectionally measured both SVV and PV in these groups using TRUS. The investigation points were pre- and post-treatment in the medical castration group and the first and second measurement in control. Measurement of PV and SV diameter and SVV was described as above.

Longitudinal Study
We prospectively assessed 7 of the 21 patients who received medical castration for more than 12 months for PSA, PV, and SVV at each period (3 to 6, 7 to 12, and 13 to 18 months).

Statistical Analysis
Statistical comparison between groups and right and left SV were done using the Mann-Whitney U-test. Those before and after treatment or the first and second measurements were done
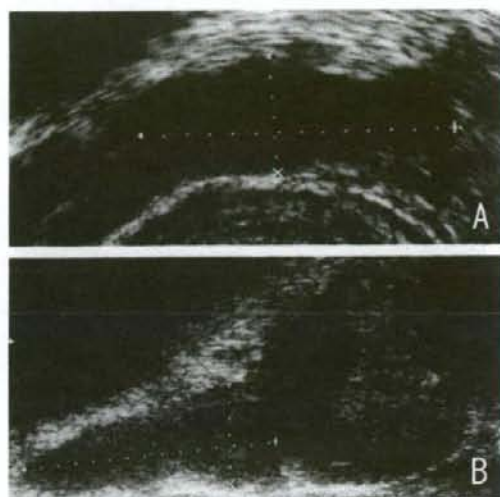

Figure 1. Demonstration of measurement of seminal vesicle with transrectal ultrasonography. **(A)** Transverse view (measurement of anterior–posterior diameter, dotted line from top to below). **(B)** Longitudinal view (measurement of lateral diameter, dotted line from left to right).

with the Wilcoxon signed-rank test. A P-value less than 0.05 was considered statistically significant.

RESULTS
Figure 2 shows typical differences of seminal vesicles images before and after medical castration. The SV size was obviously reduced after medical castration.

Table 2 shows the cross-sectional results of the volume changes of the prostate and SV. We carried out the volume calculation from the TRUS results. Although the prostate volumes were significantly different for the medical castration and control groups, both PV and SVV were significantly decreased in the medical castration group at this study point, whereas those in the control group were maintained. There were no significant differences between right and left SVV and anterior-posterior diameter of SV.

In the longitudinal assessment, every parameter including mean PSA, PV, SVV, and the anterior-posterior
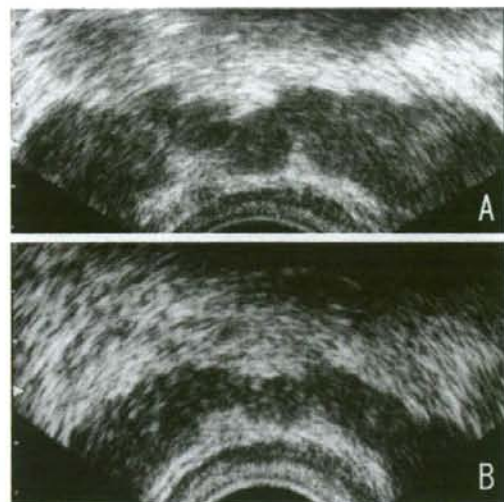
418

Figure 2. Representative TRUS images of seminal vesicles before and after medical castration. A 78-year-old T1cN0M0 prostate cancer patient. **(A)** Before medical castration. **(B)** At 8 months after medical castration.

diameter of SV was significantly reduced gradually up to 12 months after medical castration (Table 3). There was no significant difference between 7 and 12 months, and 13 and 18 months in these parameters except for SVV. The rates of reduction in the PV and SVV were 46.5% and 32.4% when comparing the baseline and 3 and 6 months, 27.0% and 30.4% comparing 3 and 6 months and 7 and 12 months, and −6.0% and 18.8% comparing 7 and 12 months and 13 and 18 months, respectively. The overall rates of reduction at 13 and 18 months after castration were 58.6% and 61.8% for PV and SVV, respectively.

COMMENT

There are many reports regarding the change of the prostate volume in prostate cancer patients after androgen ablation.[11–13] These reports were mostly associated with neoadjuvant hormonal therapy before external irradiation, brachytherapy, or radical prostatectomy. The rate of decrease has been reported to be about 30% to 40% after at least 3 months of androgen deprivation.

A longer period (8 months) of hormonal therapy was reported to be more beneficial for high-risk patients than short-term neoadjuvant androgen deprivation (3 months) before radiotherapy.[14] Thus, recently, neoadjuvant hormonal therapy is believed to be essential for high-risk prostate cancer patients. On the other hand, Liu et al. reported that long-term neoadjuvant androgen ablation before external irradiation did not increase the risk of developing gastrointestinal late toxicity.[15] Furthermore, patients with an enlarged prostate had a 2.5-fold increased risk of chronic genitourinary complications

Table 2. Cross-sectional comparison between medical castration group and controls

| | Medical Castration (21 Patients, 42 SV) | | Controls (8 Patients, 42 SV) | |
	Pre-Tx	Post-Tx	1st (After TURP)	2nd
PV (mL)	28.4 ± 9.3*†	17.0 ± 5.3†	16.6 ± 5.7*	16.5 ± 5.3
SVV (mL)	3.5 ± 1.8†	1.9 ± 1.0†	2.5 ± 1.0	2.6 ± 1.6
	(Rt; 3.4 ± 1.6, Lt; 3.5 ± 2.1)	(Rt; 1.9 ± 0.9, Lt; 1.9 ± 1.1)	(Rt; 2.4 ± 0.8, Lt; 2.7 ± 1.3)	(Rt; 2.4 ± 0.8, Lt; 2.5 ± 1.1)
Anterior-posterior diameter of SV (mm)	11.9 ± 2.9†	8.9 ± 1.9†	10.2 ± 1.8	10.0 ± 2.0
	(Rt; 11.8 ± 2.7, Lt; 12.1 ± 3.1)	(Rt; 8.8 ± 1.8, Lt; 9.1 ± 2.0)	(Rt; 9.9 ± 1.2, Lt; 10.5 ± 2.3)	(Rt; 9.8 ± 1.8, Lt; 10.4 ± 2.2)

PV, prostate volume; SVV, SV volume; other abbreviations as in Table 1.
Values are expressed as mean ± SEM.
* $P < 0.01$, Mann-Whitney U-test (medical castration group versus controls).
† $P < 0.01$ Wilcoxon signed-rank test (Pre-Tx versus Post-Tx).